

- (25) The notation is that of J. S. Griffith, "The Theory of Transition-Metal Ions", Cambridge University Press, London, 1961.
- (26) (a) D. G. Karraker, *J. Chem. Phys.*, **55**, 1084 (1971); (b) B. D. Dunlap and G. K. Shenoy, *Phys. Rev. B*, **12**, 2716 (1975).
- (27) J. E. Lowther, *Chem. Phys. Lett.*, **23**, 446 (1973).
- (28) A. J. McCaffery, J. R. Dickinson, and P. N. Schatz, *Inorg. Chem.*, **9**, 1563 (1970).
- (29) R. W. Schwartz and M. Greenblatt, *Mol. Phys.*, **29**, 97 (1975).

Contribution from the Departments of Chemistry,
University of Maine, Orono, Maine 04473, and Norwich University, Northfield, Vermont 05663

Low-Temperature Luminescence and Absorption Spectra of the d^6 Hexafluoroplatinate(IV) Ion Doped in a Cs_2GeF_6 -Type Host Lattice

HOWARD H. PATTERSON,* WILLIAM J. DeBERRY, JOSEPH E. BYRNE, MARTHA T. HSU,
and JOSEPH A. LOMENZO

Received December 13, 1976

AIC608791

The optical luminescence and absorption spectra of the $5d^6$ hexafluoroplatinate(IV) ion doped in the cubic hosts Cs_2GeF_6 , Cs_2SiF_6 , and Rb_2SiF_6 , as well as in Cs_2PtF_6 , have been measured at 20 and 2 K. Seven absorption bands with associated vibrational structures occur between 20 000 and 36 000 cm^{-1} . Electronic assignments for all of these bands have been made by means of a crystal field model with spin-orbit coupling and the relative intensities of the d-d transitions predicted with various models. The vibrational structure in the absorption bands has been assigned in terms of the PtF_6^{2-} ungerade vibrational motions. Also, luminescence has been observed for the hexafluoroplatinate ion in the host materials and in the pure material, and the vibrational structure of the luminescence band has been analyzed to give information about the change in platinum-fluorine internuclear equilibrium distance from the ground state to the excited emitting state. Finally, several conclusions are stated about d-d $t_{2g}^n \rightarrow t_{2g}^{n-1}e_g$ transitions in $5d \text{MF}_6^{2-}$ complexes.

I. Introduction

This paper reports the first high-resolution optical study of a $\text{MF}_6^{2-} 5d^n$ transition metal ion system at liquid helium temperature. We have doped the $5d^6$ hexafluoroplatinate(IV) ion in an antifluorite cubic lattice of the type Cs_2GeF_6 to the extent of about 2 mol % and measured the luminescence and absorption spectra of the complex ion between 12 000 and 50 000 cm^{-1} . The only previously reported optical studies of the hexafluoroplatinate(IV) ion have been in solution at room temperature¹ and in a CaF_2 matrix² at room temperature. For the 3d transition metal series low-temperature optical studies have been reported, for example, for (d^6) NiF_6^{2-} ,³ (d^3) CrF_6^{3-} ,⁴ and (d^3) MnF_6^{2-} .⁵

In the study of the PtF_6^{2-} ion as an impurity ion in a single Cs_2MF_6 ($M = \text{Si}, \text{Ge}$) crystal at liquid helium temperature any interactions between PtF_6^{2-} ions possibly present in the pure system have been eliminated, the PtF_6^{2-} ion is at a site of cubic symmetry, and the system is in an initial state with no excited vibrational modes. It is hoped that this will result in experimental spectra with a maximum amount of detailed information. In the analysis of the experimental data there are four objectives. First, we want to count the number of different observed electronic transitions occurring in the energy range of interest and make electronic assignments with a crystal field model. Second, we want to contrast the vibrational mode energies and geometry of the PtF_6^{2-} ion in excited electronic states with the ground state. Third, when the host lattice is changed from Cs_2GeF_6 to Cs_2SiF_6 or Rb_2SiF_6 , we want to measure the changes in the electronic and vibrational energies to understand the role of the host lattice in an electronic d-d transition. Finally, it is of interest to investigate couplings between vibrational and electronic motions of the Herzberg-Teller type to predict accurate relative intensities for d-d transitions in a $5d$ transition metal MF_6^{2-} type system.

Crystallographic studies by Sharpe⁶ have shown that Cs_2PtF_6 has the hexagonal K_2GeF_6 structure at room temperature. Also, x-ray measurements of Cs_2GeF_6 and Cs_2SiF_6 have shown that both substances have the cubic structure at

room temperature with M-F distances of 1.80 and 1.69 Å, respectively. Brown and co-workers⁷ have found that when 5% of K_2GeF_6 is doped into the K_2SiF_6 cubic host, the infrared spectrum of the mixed-crystal system shows sharp unsplit infrared peaks for the GeF_6^{2-} species characteristic of cubic site symmetry. Thus, when Cs_2PtF_6 is doped to the extent of 1-5 mol % in the cubic hosts Cs_2SiF_6 and Cs_2GeF_6 , the observed optical spectrum should be for an octahedral PtF_6^{2-} species with cubic site symmetry. The optical studies of Helmholtz and Russo⁵ on Cs_2MnF_6 in Cs_2GeF_6 have shown that Cs_2GeF_6 does not absorb up to 2500 Å. Our studies for Cs_2GeF_6 and Cs_2SiF_6 are in agreement with their work.

II. Experimental Section

Cs_2PtF_6 was prepared by fluorinating Cs_2PtCl_6 with BrF_3 as the fluorinating agent, according to a procedure given in ref 8. A Teflon reaction vessel was used for the preparation to minimize any contamination from the SiF_6^{2-} ion. The product was recrystallized from hot water.

The Cs_2GeF_6 used in this study was obtained from Alfa Inorganics and used without further purification. The Cs_2SiF_6 was prepared by mixing a solution of 30% H_2SiF_6 with a concentrated solution of CsF containing the proper stoichiometric amount of the salt. The precipitated Cs_2SiF_6 was washed and then dried in a stream of nitrogen gas.

Mixed crystals of Cs_2PtF_6 with Cs_2SiF_6 , Cs_2GeF_6 , or Rb_2SiF_6 were grown from a solution which initially contained about 0.1 g of Cs_2PtF_6 and about 0.2 g of host material dissolved in a minimum amount of 49% hydrofluoric acid at 60 °C. The solution was filtered and placed in a Teflon beaker at 60 °C and cooled slowly. Mixed crystals were harvested in 4-7 days. The crystals were 1-2 mm across a face and were yellow.

A selected number of the mixed crystals were analyzed by atomic absorption spectroscopy to determine the mole percent of platinum complex in the mixed crystals by techniques previously reported.⁹ The crystals were found to contain 1-2 mol % of Cs_2PtF_6 . Also, the Cs_2PtF_6 - Cs_2GeF_6 mixed crystals were analyzed for contamination of SiF_6^{2-} by infrared spectroscopy using a KBr mull and found to not contain any measurable amount of SiF_6^{2-} .

Infrared measurements between 250 and 4000 cm^{-1} were carried out at room temperature with a Perkin-Elmer Model 457 spectrophotometer. Raman studies at room temperature were done with a Cary Model 81 spectrometer. The optical measurements at liquid

* To whom correspondence should be addressed at the University of Maine.

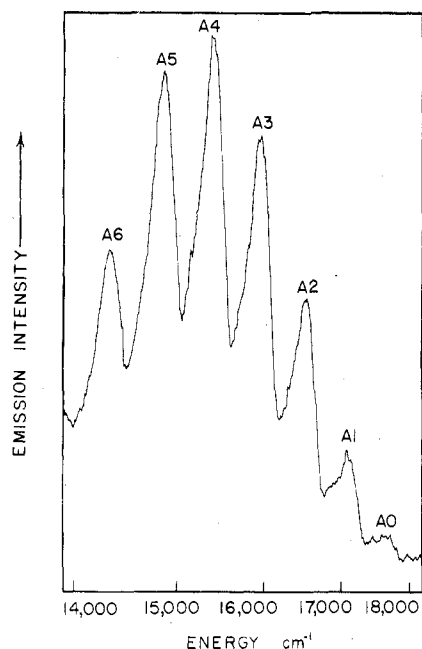


Figure 1. Luminescence spectrum of a single Cs_2PtF_6 crystal at liquid hydrogen temperature.

Table I. Summary of the Hexafluoroplatinate(IV) Ion Room-Temperature Solution and Solid-State Spectra

Band	Soln results ¹		Solid-state results ² Energy, cm^{-1}
	Energy, cm^{-1}	Oscillator strength	
I	22 500	6×10^{-5}	21 000–28 000
II	24 400	10×10^{-5}	21 000–28 000
III	31 400	70×10^{-5}	32 500
IV	36 400	60×10^{-5}	37 000

hydrogen temperature were made with a McPherson Model 2051 monochromator using a PAR Model 124A Lock-In and photomultiplier detector, with cooling achieved by a Model AC-3L Cryo-Tip. The optical experiments at 2 K were carried out as described previously.⁹

III. Results

Luminescence Spectra. At liquid hydrogen temperature, the luminescence spectra of the hexafluoroplatinate(IV) ion doped in the Cs_2GeF_6 host or the Cs_2SiF_6 host are very similar with no measured differences detected for the vibronic peak energies. However, if the host is changed from Cs_2SiF_6 to Rb_2SiF_6 , the band maximum increases by 390 cm^{-1} and the energy separation between the members of the progression increases by about 10 cm^{-1} to become 580 cm^{-1} . Finally, the luminescence spectrum of a pure Cs_2PtF_6 crystal at liquid hydrogen temperature is shown in Figure 1. In this case, the band maximum is 810 cm^{-1} greater than the mixed Cs_2SiF_6 or Cs_2GeF_6 case, and the separation between the peaks is the same as for the Rb host.

When the temperature of a Cs_2PtF_6 - Cs_2GeF_6 (see Figure 2) or a pure Cs_2PtF_6 crystal is lowered from liquid hydrogen temperature ($\sim 20 \text{ K}$) to 2 K, small B peaks appear in the luminescence spectrum between the A peaks. On the other hand, as the temperature is raised from 20 K to liquid nitrogen temperature, the A peaks decrease in height and broaden in width. At room temperature, the broad luminescence band is symmetrically shaped with no structure. The intensity of luminescence from a 2% Cs_2PtF_6 - Cs_2GeF_6 mixed crystal is about the same as from a pure Cs_2PtF_6 crystal.

Electronic Absorption Spectra. In Table I the solution spectrum of the hexafluoroplatinate(IV) ion at room temperature is summarized. Our experimental data are in

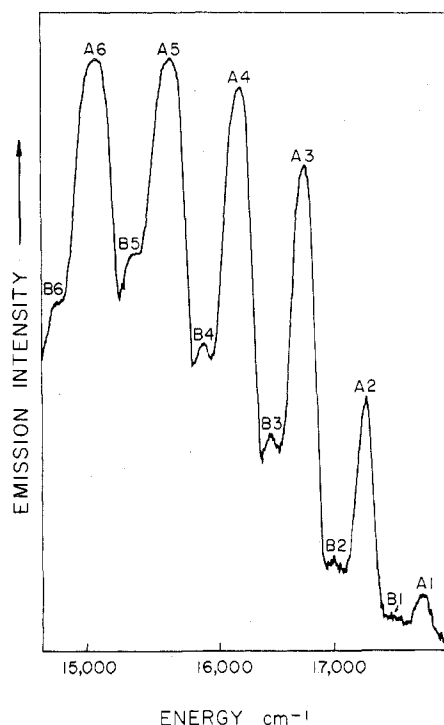


Figure 2. Microphotometer tracing of a photographic plate showing the luminescence spectrum of a Cs_2PtF_6 - Cs_2GeF_6 crystal at 2 K.

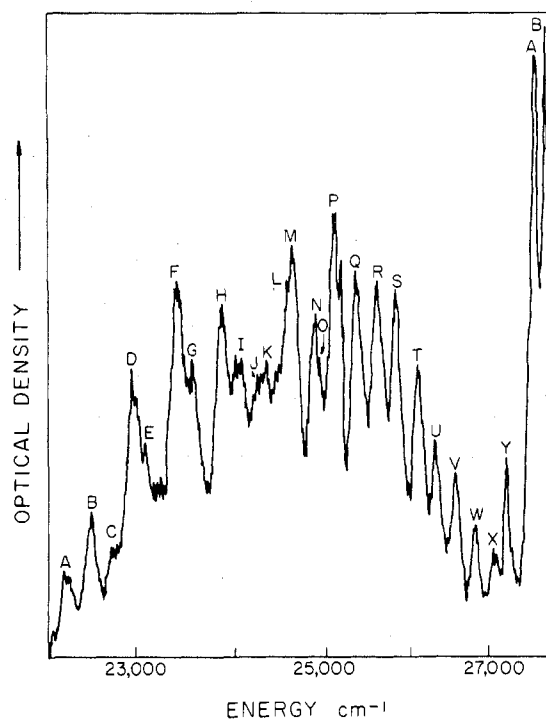


Figure 3. Microphotometer tracing of a photographic plate showing the absorption spectrum of a Cs_2PtF_6 - Cs_2GeF_6 crystal between $22\,000$ and $28\,000 \text{ cm}^{-1}$ at 2 K.

agreement with the Jorgensen results,¹ except that we are unable to distinguish between the Jorgensen bands I and II. Also, in Table I the room-temperature solid spectrum of Brown et al.² for Cs_2PtF_6 is given. Our data are in agreement.

The electronic absorption spectrum of a Cs_2PtF_6 - Cs_2GeF_6 single crystal at 2 K is shown in Figures 3–5, and the energies of the various peaks are given in Table II. In particular, in Figure 3 the absorption spectrum of the hexafluoroplatinate(IV) ion is shown between $22\,000$ and $28\,000 \text{ cm}^{-1}$. In

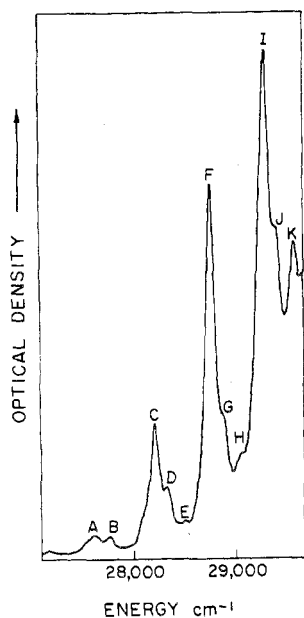


Figure 4. Absorption spectrum of a $\text{Cs}_2\text{PtF}_6\text{-Cs}_2\text{GeF}_6$ crystal between 27 000 and 30 000 cm^{-1} at 2 K using photographic plates as a means of detection.

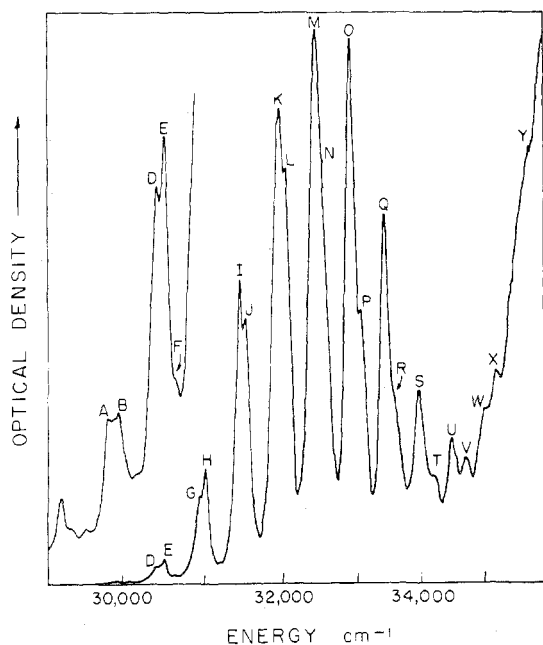


Figure 5. Absorption spectrum of the PtF_6^{2-} ion in a Cs_2GeF_6 host lattice at 2 K showing the $\Gamma_1(^1A_{1g}) \rightarrow \Gamma_4(^1T_{1g})$ transition and the beginning of the $\Gamma_1(^1A_{1g}) \rightarrow \Gamma_5(^1T_{2g})$ transition.

this energy interval more than one electronic transition is expected from crystal field theory. On the basis of relative intensities, it is reasonable to say that peaks Y, A, and B correspond to a separate electronic transition from, for example, peaks U, V, W.

In Figure 4 the PtF_6^{2-} absorption spectrum is shown between 27 000 and 30 000 cm^{-1} . Note that peaks A and B of Figure 3 correspond to peaks A and B of Figure 4. In Figure 5, the $\text{Cs}_2\text{PtF}_6\text{-Cs}_2\text{GeF}_6$ absorption spectrum is given between 29 000 and 36 000 cm^{-1} . Beyond 36 000 cm^{-1} the quartz optics begins to absorb.

IV. Assignment of Electronic Transitions

Crystal Field Model. Platinum(IV) has a $5d^6$ electronic configuration. In a crystal field of octahedral symmetry a d^6

Table II. Observed Optical Transitions for a $\text{Cs}_2\text{PtF}_6\text{-Cs}_2\text{GeF}_6$ Crystal at 2 K

Peak no.	Energy, cm^{-1}	Assignment
3-A	22 440	$\Gamma_3(^3T_{1g}) + \nu_6 + 6\nu_1$
B	22 580	$+ \nu_4 + 6\nu_1$
C	22 785	$+ \nu_3 + 6\nu_1$
D	22 990	$\Gamma_5(^3T_{1g}) + \nu_3 + n\nu_1$
E	23 120	$+ \nu_6 + (n+1)\nu_1$
F	23 420	$+ \nu_3 + (n+1)\nu_1$
G	23 595	$+ \nu_6 + (n+2)\nu_1$
H	23 880	$+ \nu_3 + (n+2)\nu_1$
I	24 070	$+ \nu_6 + (n+3)\nu_1$
K	24 350	$+ \nu_3 + (n+3)\nu_1$
L	24 600	$+ \nu_6 + (n+4)\nu_1$
M	24 650	$\Gamma_4(^3T_{1g}) + \nu_4 + n\nu_1$
N	24 900	$+ \nu_3 + n\nu_1$
O	24 945	
P	25 120	$+ \nu_4 + (n+1)\nu_1$
Q	25 360	$+ \nu_3 + (n+1)\nu_1$
R	25 610	$+ \nu_4 + (n+2)\nu_1$
S	25 835	$+ \nu_3 + (n+2)\nu_1$
T	26 110	$+ \nu_4 + (n+3)\nu_1$
U	26 335	$+ \nu_3 + (n+3)\nu_1$
V	26 580	$+ \nu_4 + (n+4)\nu_1$
W	26 830	$+ \nu_3 + (n+4)\nu_1$
X	27 090	$\Gamma_4(^3T_{1g}) + \nu_3 + n\nu_1$
Y	27 250	$+ \nu_6 + (n+1)\nu_1$
4-A	27 650	$\Gamma_4(^3T_{1g}) + \nu_3 + n\nu_1$
B	27 790	$+ \nu_6 + (n+1)\nu_1$
	27 950	$+ \nu_4 + (n+1)\nu_1$
C	28 210	$+ \nu_3 + (n+1)\nu_1$
D	28 320	$+ \nu_6 + (n+2)\nu_1$
E	28 500	$+ \nu_4 + (n+2)\nu_1$
F	28 760	$+ \nu_3 + (n+2)\nu_1$
G	28 890	$+ \nu_6 + (n+3)\nu_1$
H	29 060	$+ \nu_4 + (n+3)\nu_1$
I	29 300	$+ \nu_3 + (n+3)\nu_1$
J	29 420	$+ \nu_6 + (n+4)\nu_1$
K	29 600	$+ \nu_4 + (n+4)\nu_1$
5-A	29 850	$\Gamma_4(^1T_{1g}) + \nu_3 + n\nu_1$
B	29 960	$+ \nu_6 + (n+1)\nu_1$
C	30 175	$\Gamma_5(^3T_{2g}) + \nu_{\text{odd}} + n\nu_1$
D	30 420	$\Gamma_4(^1T_{1g}) + \nu_3 + (n+1)\nu_1$
E	30 510	$+ \nu_6 + (n+2)\nu_1$
F	30 660	$\Gamma_5(^3T_{2g}) + \nu_{\text{odd}} + (n+1)\nu_1$
G	30 950	$\Gamma_4(^1T_{1g}) + \nu_3 + (n+2)\nu_1$
H	31 030	$+ \nu_6 + (n+3)\nu_1$
I	31 480	$+ \nu_3 + (n+3)\nu_1$
J	31 560	$+ \nu_6 + (n+4)\nu_1$
K	31 930	$+ \nu_3 + (n+4)\nu_1$
L	32 090	$+ \nu_6 + (n+5)\nu_1$
M	32 450	$+ \nu_3 + (n+5)\nu_1$
N	32 625	$+ \nu_4 + (n+6)\nu_1$
O	33 010	$+ \nu_3 + (n+6)\nu_1$
P	33 160	$+ \nu_4 + (n+7)\nu_1$
Q	33 500	$+ \nu_3 + (n+7)\nu_1$
R	33 670	$+ \nu_4 + (n+8)\nu_1$
S	34 000	$+ \nu_3 + (n+8)\nu_1$
T	34 270	$\Gamma_5(^1T_{2g}) + n\nu_1 + \nu_{\text{odd}}$
U	34 510	$\Gamma_4(^1T_{1g}) + (n+9)\nu_1 - \nu_3$
V	34 760	$\Gamma_5(^1T_{2g}) + (n+1)\nu_1 + \nu_{\text{odd}}$
W	35 040	$\Gamma_4(^1T_{1g}) + (n+10)\nu_1 + \nu_3$
X	35 220	$\Gamma_5(^1T_{2g}) + (n+2)\nu_1 + \nu_{\text{odd}}$

electronic configuration gives the terms

$$t_{2g}^6: ^1A_1$$

$$t_{2g}^5e_g: ^3T_1 + ^3T_2 + ^1T_1 + ^1T_2$$

It is expected that spin-orbit interaction will be important for the $5d$ transition metal series and be sufficiently large ($\sim 2500 \text{ cm}^{-1}$)^{10,11} that it cannot be treated by perturbation theory. The effect of spin-orbit interaction is to couple the spin and angular momentum states together to give resulting states transforming as Γ_7 of the octahedral point group. When referring to the

Table III. Comparison of the Observed and Calculated Energies for the Optical Absorptions of PtF₆²⁻ in Cs₂GeF₆ at 2 K^{a,b}

Level	Energy, cm ⁻¹		Composition of levels	Probability		Calcd oscillator strength	
	Calcd	Obsd		JPD ¹⁵	Spin ¹¹	JPD ¹⁵	Spin ^{11,c}
Γ ₅	37 080	37 000	88.9% ¹ T ₂ , 5.3% ³ T ₁ , 3.8% ³ T ₂ , 1.2% ³ E	79.3W	0.82	60 × 10 ⁻⁶	60 × 10 ⁻⁶
Γ ₄	32 530	32 450	71.3% ¹ T ₁ , 25.4% ³ T ₂ , 1.9% ³ T ₁ , 1.1% ⁵ T ₂	64.4V	0.67	70 × 10 ⁻⁶	49 × 10 ⁻⁶
Γ ₂	31 770		99.2% ³ T ₂ , 0.8% ¹ A ₂	0	0.09	0	2 × 10 ⁻⁶
Γ ₅	30 950	30 660	86.8% ³ T ₂ , 9.6% ³ T ₁ , 2.3% ⁵ T ₂ , 0.6% ¹ T ₂	0.1W	0.09	0.1 × 10 ⁻⁶	6 × 10 ⁻⁶
Γ ₃	30 100		67.4% ³ T ₂ , 31.4% ³ T ₁ , 0.7% ¹ E	0	0.09	0	2 × 10 ⁻⁶
Γ ₄	29 070	29 300	56.2% ³ T ₁ , 31.6% ³ T ₂ , 8.4% ¹ T ₁ , 3.5% ⁵ T ₂	7.3V	0.15	8 × 10 ⁻⁶	11 × 10 ⁻⁶
Γ ₁	28 625		82.0% ³ T ₁ , 9.8% ¹ A ₁ , 8.0% ⁵ T ₂	0	0.16	0	4 × 10 ⁻⁶
Γ ₄	24 280	25 118	39.8% ³ T ₂ , 39.4% ³ T ₁ , 16.0% ¹ T ₁ , 4.2% ⁵ T ₂	14.1V	0.22	15 × 10 ⁻⁶	16 × 10 ⁻⁶
Γ ₅	23 940	23 418	83.1% ³ T ₁ , 8.2% ³ T ₂ , 5.4% ¹ T ₂ , 3.0% ⁵ T ₂	3.8W	0.13	3 × 10 ⁻⁶	10 × 10 ⁻⁶
Γ ₃	23 000	22 579	66.8% ³ T ₁ , 28.0% ³ T ₂ , 3.8% ⁵ T ₂ , 1.4% ¹ E	0	0.10	0	5 × 10 ⁻⁶
Γ ₁	0.0	0.0	91.2% ¹ A ₁ , 8.7% ³ T ₁	0			

^a For $B = 395$, $C = 2254$, $\lambda_{so} = -3579$, $Dq = -3150$ cm⁻¹. ^b The calculated oscillator strengths should be compared with the experimental data in Table I. ^c The excited state degeneracy has been included and these predicted values have been normalized to the experimental 37 000-cm⁻¹ band oscillator strength.

Γ₇ irreducible representations, we shall use the Bethe notation Γ_{*i*}, where in this even-electron case, $i = 1-5$.

Schroeder¹¹ has calculated the complete matrices of the spin-orbit interaction for the d⁶ configuration in a strong cubic field scheme. The phases of the Schroeder spin-orbit matrix elements are such that they can be added directly to the electrostatic and cubic field matrices of Tanabe and Sugano¹² to give the complete energy matrices. The energy matrices are a function of four parameters: B and C , the Racah parameters which describe interelectronic repulsion; $10Dq$, the crystal field parameter; and λ , the spin-orbit parameter. A computer program has been used to compute the energies and composition of the Γ_{*i*} states for selected values of the parameters B , C , $10Dq$, and λ .

The assignment of the excited electronic states was carried out in three steps. In the first step, it was recognized that in the Tanabe-Sugano limit of zero spin-orbit interaction, two spin-allowed transitions ($t_{2g}^6, {}^1A_1 \rightarrow t_{2g}^5e_g^1, {}^1T_1$ and 1T_2) and two spin-forbidden transitions ($t_{2g}^6, {}^1A_1 \rightarrow t_{2g}^5e_g^1, {}^3T_1$ and 3T_2) should occur. When the spin-orbit interaction is turned on, the 3T_1 and 3T_2 states give rise to eight resulting states with some spin-singlet character. Bands I and II in Table I were assigned to the two spin-forbidden transitions while bands III and IV were assigned as the eight spin-allowed transitions. From these assignments the crystal field parameter, $10Dq$, was estimated to be about 30 000 cm⁻¹.

In the second step, for $10Dq = 30 000$ cm⁻¹ and $\lambda = 2500$ cm⁻¹, a wide range of B and C combinations was used to find reasonable values of these parameters which would give the correct energy separation between Γ₄(¹T₁), Γ₅(¹T₂), and the Γ₁(¹A_{1g}) ground state. The values for the B and C parameters were 300 and 1800 cm⁻¹, respectively. In the final step, a least-squares computer program was used to give the best calculated fit to the experimental data.

In Table III the calculated and observed energies are given for the case where the observed experimental maxima have been fit to the crystal field model. This corresponds to the situation where an electronic transition takes place without any change in the Pt-F internuclear distance. The listed parameters for the hexafluoroplatinate(IV) ion can be compared with the values reported for K₂NiF₆³ ($B = 485$, $C = 2425$, $10Dq = 20900$, and $\lambda = 0$ cm⁻¹) or for K₃IrCl₆¹¹ ($B = 338$, $C = 1520$, $10Dq = 22750$, and $\lambda = 2820$ cm⁻¹).

Molecular Orbital Model. Cotton and Harris¹³ have reported a semiempirical extended Hückel calculation for the PtCl₆²⁻ ion. From the data in Moore's tables¹⁴ and other molecular orbital calculations we can estimate the valence-state ionization potentials (VSIP) (2s, 2p) for the fluoride ligand. If we compare the 2s, 2p VSIP values for F with the Cl values, we can predict without a detailed calculation the ordering of the energy levels and their separations. This is done in Figure

6. For fluorine the ligand orbitals and the metal orbitals are separated to a greater extent than for Cl or Br with the result that ligand to metal charge-transfer transitions occur at much greater energies than d-d transitions for PtF₆²⁻ and other 5d MF₆²⁻ complexes. In contrast, for PtCl₆²⁻ the Cotton and Harris¹³ MO calculation predicts a $t_{2g} \rightarrow e_g$ separation of 35 000 cm⁻¹ and a $t_{2u} \rightarrow t_{2g}$ separation of 44 000 cm⁻¹. This means that in 5d MCl₆²⁻ octahedral complexes d-d and ligand-metal transitions will appear at about the same energies and it will be difficult to identify the weaker parity-forbidden d-d transitions; however, in the corresponding fluoride complexes the d-d transitions can be studied without this problem.

Intensity Model to Describe d-d Transitions. The simplest model to describe the relative intensities of d-d electronic transitions involves considering only the spin-allowedness of a transition. Thus, if the ground state is pure singlet spin and an excited state pure singlet, the transition probability is 100 while a transition to a pure triplet state is zero. By use of this approach the relative intensities of the d-d electronic transitions for PtF₆²⁻ have been calculated and are listed in Table III. This picture has been suggested by Schroeder¹¹ previously for K₃IrCl₆.

A second model for estimating the relative intensities of Laporte-forbidden d-d transitions is that of Jordan, Patterson, and Dorain¹⁵ (JPD). They considered vibronically allowed electric dipole transitions in octahedral complexes with spin-orbit coupling. In O_h symmetry, both the initial and final electronic states are gerade, so the intensity results from vibronic coupling with ungerade ligand states of the type $t_{1u}^5e_g^1$ or $t_{2u}^5e_g^1$. This model predicts for a d⁶ system that transitions to Γ₁, Γ₂, or Γ₃ states should be much weaker than transitions to Γ₄ or Γ₅ electronic states. Transitions to Γ₄ or Γ₅ final electronic states can be expressed, respectively, as a number calculated from the crystal field eigenfunctions times an irreducible matrix element V or W . The results of this model are given in Table III. If V is set equal to 1.09×10^{-5} and W is set equal to 0.76×10^{-5} , so that the relative transition probabilities for the transitions at 37 000 and 32 450 cm⁻¹ are set equal to the experimental oscillator strengths, then the model predicts lower energy transitions in qualitative agreement with the experimental data, as shown in Table III.

In comparison of the Schroeder and the JPD intensity model predictions of Table III with the available experimental low-temperature data two points should be made. First, the JPD model indicates the correct number of observed transitions in a given energy range while the spin-intensity model predicts all transitions should be observable. Second, because of the approximations in the model, the JPD model can only serve as a qualitative guide to the analysis of experimental data for d-d transitions in other octahedral systems.

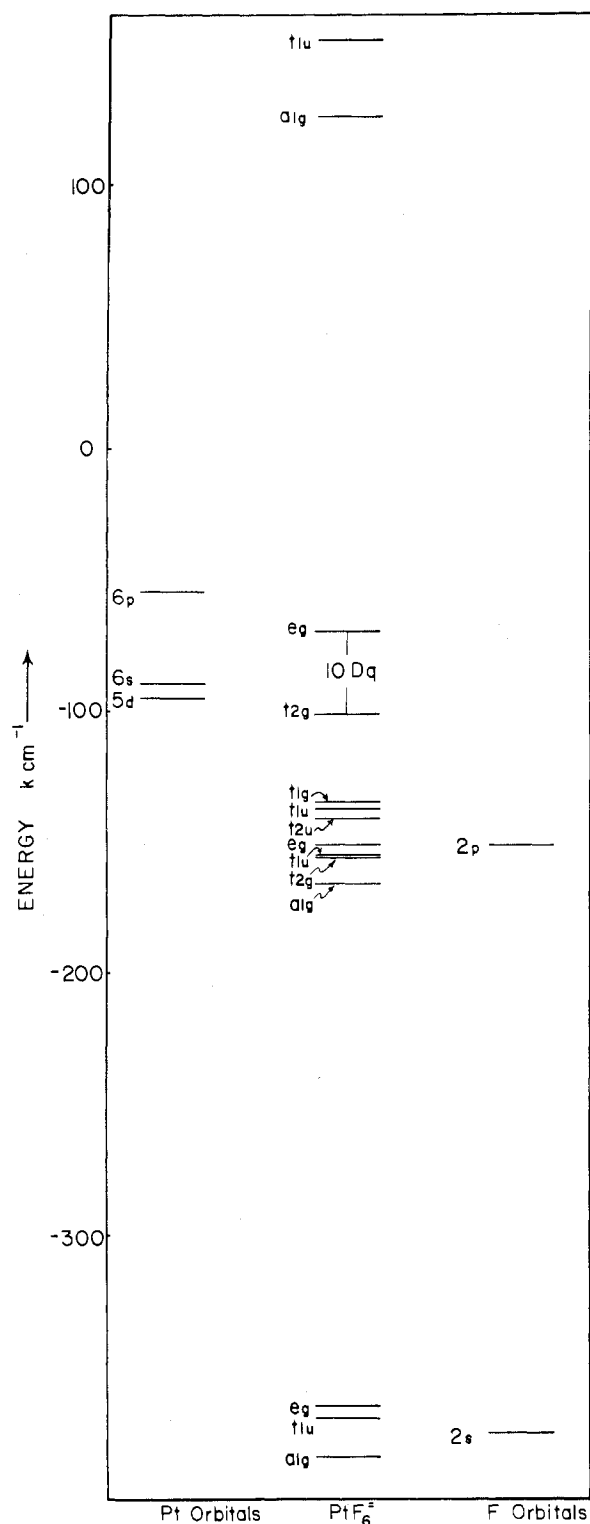


Figure 6. Molecular orbital energy level diagram for the PtF_6^{2-} complex ion.

V. Assignment of Vibrational Structure

Predicted Pattern. To assign the vibrational structure associated with each electronic transition we must consider the normal modes of vibration of the PtF_6^{2-} octahedral complex ion. They can be denoted¹⁶ as $\nu_1(a_{1g})$, $\nu_2(e_g)$, $\nu_3(t_{1u})$, $\nu_4(t_{1u})$, $\nu_5(t_{2g})$, and $\nu_6(t_{2u})$, where the irreducible representation of the O_h point group, according to how the vibrational mode transforms, is given within the parentheses. Woodward and Ware¹⁷ (WW) have measured the room-temperature infrared spectrum of Cs_2PtF_6 as Nujol mulls and KBr pressed disks

and the Raman spectrum of PtF_6^{2-} in aqueous solution. They reported that $\nu_1 = 600 \text{ cm}^{-1}$, $\nu_2 = 576 \text{ cm}^{-1}$, $\nu_3 = 571 \text{ cm}^{-1}$, $\nu_4 = 281 \text{ cm}^{-1}$, and $\nu_5 = 210 \text{ cm}^{-1}$. The ν_6 mode is inactive but a weak combination IR band observed at 719 cm^{-1} was assigned by WW to $\nu_2 + \nu_6$ to give a value of 143 cm^{-1} for ν_6 . Raman experiments at 6 K for Cs_2SiF_6 , for example, indicate that the internal mode bending and stretching vibrational mode energies change less than 5 cm^{-1} from room temperature to 6 K.

We have prepared pure thin disks of Cs_2PtF_6 to measure the combination bands in the infrared region. The fundamental peaks are broad at room temperature but the combination bands are sharp and distinct. We observe a relatively sharp peak at 719 cm^{-1} and again assign it to $\nu_2 + \nu_6$. Further, we have measured the Raman spectrum of a single Cs_2PtF_6 crystal at room temperature and found $\nu_1 = 590 \text{ cm}^{-1}$, $\nu_2 = 567 \text{ cm}^{-1}$, and $\nu_5 = 225 \text{ cm}^{-1}$; thus, ν_6 is equal to 152 cm^{-1} . The Raman spectrum of a mixed $\text{Cs}_2\text{PtF}_6\text{-Cs}_2\text{GeF}_6$ room-temperature crystal, when excited by 4880-\AA laser light, shows a resonance Raman effect for the PtF_6^{2-} ion with the ν_1 , ν_2 , ν_5 peaks very intense and no evidence of the Cs_2GeF_6 host Raman fundamental peaks. This is interesting because previous Raman studies¹⁸ have shown that the $d^8 \text{PdX}_4^{2-}$ ($X = \text{Cl, Br, I}$) ions in this excitation wavelength range show the antiresonance Raman effect.

Standard group theory¹⁶ for d-d transitions in a PtF_6^{2-} octahedral complex gives the result that the vibronic pattern should consist of $(\nu_6, \nu_4, \nu_3) + n\nu_1$ peaks, with possibly weaker peaks due to the coupling of the complex to the lattice motions. The lattice vibration peaks should be much weaker than the ν_6, ν_4, ν_3 peaks because these vibrations will be much less effective in destroying the center of symmetry than the internal odd modes themselves. The energy separation between peaks of similar appearance in the PtF_6^{2-} absorption spectrum is about 500 cm^{-1} , and if this energy is assigned to the excited-state a_{1g} mode, then this represents a reduction of 15% from the ground-state value. Thus, we may expect a difference as large as 15% for the excited-state vibrational mode energies vs. the ground-state room-temperature values.

In order to assign the experimental absorption spectrum of PtF_6^{2-} to different electronic transitions three criteria were used: (1) predictions of crystal field theory for a given spectral region; (2) the difference in appearance between spectral peaks as observed by the eye on the original photographic plates; (3) energy differences between adjacent peaks.

Assignment of Vibronic Structure. In the region of $30\,000\text{-}40\,000 \text{ cm}^{-1}$ the $\Gamma_1(^1A_{1g}) \rightarrow \Gamma_4(^1T_{1g})$ and the $\Gamma_1(^1A_{1g}) \rightarrow \Gamma_5(^1T_{2g})$ transitions should occur with appreciable intensity. For the spectrum shown in Figure 5, if the energy differences between adjacent peaks are compared with the ν_6, ν_4, ν_3 energy differences, the most reasonable assignments are those listed in Table II. At the beginning of the transition, the ν_6 mode is the most intense, but by the Franck-Condon maximum the ν_3 mode has become the most intense, and at peak P the ν_4 mode shows intensity. From the crystal field calculations the C and F peaks can be assigned to the relatively weak $\Gamma_1(^1A_{1g}) \rightarrow \Gamma_5(^3T_{2g})$ transition. At about $34\,000 \text{ cm}^{-1}$ a new set of peaks (T, V, X) appear with increasing intensity and are assigned to the $\Gamma_1(^1A_{1g}) \rightarrow \Gamma_5(^1T_{2g})$ transition.

The transition shown in Figure 4 is characterized by the appearance of the ν_6, ν_4, ν_3 modes. Again, the ν_3 mode is the most intense and ν_4 is the least intense ungerade mode.

For the spectrum between $22\,000$ and $27\,000 \text{ cm}^{-1}$ shown in Figure 3, a large number of peaks appear. The crystal field and JPD intensity calculations predict two transitions with some intensity ($\Gamma_1(^1A_{1g}) \rightarrow \Gamma_5(^3T_{1g})$ and $\Gamma_1(^1A_{1g}) \rightarrow \Gamma_4(^3T_{2g})$) and these are assigned respectively to peaks D-L and M-W. For the first transition the $(n\nu_1 + \nu_3)$ mode has the most

intensity but for the second transition the ($\nu_1 + \nu_4$) mode is the most intense. The three peaks A, B, C are assigned to the $\Gamma_1(^1A_{1g}) \rightarrow \Gamma_3(^3T_{1g})$ transition and are relatively weak; the ν_4 mode in this case is the most intense.

VI. Discussion of Luminescence Band

The 2-K luminescence spectra of a $\text{Cs}_2\text{PtF}_6\text{-Cs}_2\text{GeF}_6$ crystal and a pure Cs_2PtF_6 crystal both show more resolved vibrational structure than in previously reported K_2PtCl_6 , K_2PtBr_6 , and K_2PtI_6 luminescence studies.¹⁹ The vibronic peaks can be assigned by considering the average energy separation between the adjacent A and B peaks. If the A peaks are assigned to a progression in $\nu_1 + \nu_4$ and the B peaks to a progression in $\nu_1 + \nu_3$, the ($\nu_3 - \nu_4$) calculated difference is 292 cm^{-1} in comparison to the room-temperature infrared ($\nu_3 - \nu_4$) difference of 290 cm^{-1} .

In the $\text{K}_2\text{PtCl}_6\text{-K}_2\text{SnCl}_6$ system,¹⁹ the maximum of the luminescence band is at $14\,500\text{ cm}^{-1}$ with a 300-cm^{-1} progression. The lowest absorption band occurs at $18\,300\text{ cm}^{-1}$ to give a Stokes shift of 3800 cm^{-1} . For the $\text{Cs}_2\text{PtF}_6\text{-Cs}_2\text{GeF}_6$ system, where the average ν_1 in the luminescence band is 560 cm^{-1} , this corresponds to a Stokes shift of $3800 \times (560/360)$ or 7100 cm^{-1} . Further, if the lowest energy absorption maximum is at $22\,579\text{ cm}^{-1}$, then the luminescence maximum is predicted to be at about $15\,500\text{ cm}^{-1}$. The experimental maximum is observed at $16\,170\text{ cm}^{-1}$ or about 680 cm^{-1} from the predicted value, which corresponds to a single ν_1 quantum difference. This may indicate that the d-state potential energy surfaces in the Cs_2PtCl_6 and Cs_2PtF_6 systems are similar.

In the $\text{Cs}_2\text{PtF}_6\text{-Cs}_2\text{GeF}_6$ system, if the 0-0 energy is taken to be the average of the absorption and luminescence maxima, $19\,375\text{ cm}^{-1}$, the ν_4 mode should appear at $19\,094\text{ cm}^{-1}$, $\nu_4 + \nu_1$ should appear at $18\,532\text{ cm}^{-1}$, and so on. In the experimental luminescence $\text{Cs}_2\text{PtF}_6\text{-Cs}_2\text{GeF}_6$ spectrum, the first peak appears with high sensitivity at $18\,416\text{ cm}^{-1}$ and is thus assigned as ($\nu_4 + \nu_1$).

If the host lattice is changed from Cs_2SiF_6 to Rb_2SiF_6 , the luminescence band maximum increases by 390 cm^{-1} ; this can be interpreted as arising from a smaller lattice constant (8.45 to 8.09 \AA or 4% decrease) and a greater $10Dq$ value of about 4%. In contrast, a change of host from Cs_2SiF_6 to Cs_2GeF_6 means a lattice constant change from $a_0 = 8.89$ to $a_0 = 8.99$ or a 1% change with the result that there is no measured difference in the luminescence A peak energies. Finally, if a pure Cs_2PtF_6 crystal is compared with a $\text{Cs}_2\text{PtF}_6\text{-Cs}_2\text{GeF}_6$ or $\text{Cs}_2\text{PtF}_6\text{-Cs}_2\text{SiF}_6$ crystal, it is found that the pure crystal luminescence maximum is 810 cm^{-1} greater than in the mixed crystals. This is probably related to the fact that in the pure Cs_2PtF_6 the site symmetry of the anion is D_{3d} rather than O_h and PtF_6^{2-} is constrained more by the Cs^+ cations, which results in a larger $10Dq$. The fact that the pure Cs_2PtF_6 material shows no splitting of the ν_4 peak observed in luminescence at 2 K would indicate that the distortion of the PtF_6^{2-} entity from O_h symmetry is slight.

The Franck-Condon principle^{20,21} governs the relative transition probabilities for luminescence from $v' = 0$ of an excited electronic state to the various vibrational v'' levels of the ground state. As we have previously discussed²⁰ for PtCl_4^{2-} , one can calculate Franck-Condon factors as a function of molecular geometry and, by fitting the relative intensities of the individual components in the luminescence band to the calculated intensities, determine the difference in Pt-F

equilibrium separation, Δ , between the initial excited state and the final ground state. The result of the computer calculation²² is that for both Cs_2PtF_6 (pure) and the mixed $\text{Cs}_2\text{PtF}_6\text{-Cs}_2\text{GeF}_6$ and $\text{Cs}_2\text{PtF}_6\text{-Cs}_2\text{SiF}_6$ systems Δ is 0.20 \AA , but for the rubidium case, $\text{Rb}_2\text{PtF}_6\text{-Rb}_2\text{SiF}_6$, $\Delta = 0.23\text{ \AA}$. The physical interpretation of these results is that (1) there is a large change in the ν_1 vibrational energy from the ground state to the $t_{2g}^5 e_g$ excited states (25%) and a change of 0.20 \AA in equilibrium separation, meaning that it is virtually impossible to observe absorption origins, and (2) variation of cation from Cs^+ to Rb^+ results in a contraction of the Pt-F separation in the ground state but not necessarily in the excited state, where the electronic density is partially on the ligand orbitals.

VII. Conclusions

It has been shown in this paper that the optical absorption and luminescence spectra of the $5d^6$ hexafluoroplatinate(IV) ion at 2 K can be understood on the basis of a crystal field model with spin-orbit coupling. Also, it has been shown that the vibronic intensity model of JPD for d-d transitions in octahedral complexes is useful for assigning transitions in regions where there are many possible transitions. The final conclusion from our luminescence analysis is that d-d $t_{2g}^n \rightarrow t_{2g}^{n-1} e_g$ type transitions in 5d transition metal complexes show long Franck-Condon progressions with a considerable change in equilibrium internuclear separation between the ground and excited electronic states. Thus, it is extremely likely that the first observed peak in an absorption band will involve several quanta of a_{1g} vibration.

Registry No. PtF_6^{2-} , 16871-53-7; Cs_2PtF_6 , 16923-85-6; Cs_2GeF_6 , 16919-21-4; Cs_2SiF_6 , 16923-87-8; Rb_2SiF_6 , 16925-27-2.

References and Notes

- (1) C. K. Jorgensen, *Acta Chem. Scand.*, **12**, 1539 (1958), *Adv. Chem. Phys.*, **5**, 118 (1963).
- (2) D. H. Brown, D. R. Russell, and D. W. A. Sharp, *J. Chem. Soc. A*, **18** (1966).
- (3) M. J. Reissfeld, L. B. Asprey, and R. A. Penneman, *J. Mol. Spectrosc.*, **29**, 109 (1969). For other references to MF_6^{n-} optical studies, the reader should see A. B. P. Lever, "Inorganic Electronic Spectroscopy", Elsevier, 1968.
- (4) H. L. Schlafer, H. Gausmann, and H. U. Zander, *Inorg. Chem.*, **6**, 1528 (1967).
- (5) L. Helmholz and M. E. Russo, *J. Chem. Phys.*, **59**, 5455 (1973).
- (6) A. G. Sharpe, *J. Chem. Soc.*, **197** (1953).
- (7) D. H. Brown, K. R. Dixon, C. M. Livingston, R. H. Nuttall, and D. W. A. Sharp, *J. Chem. Soc. A*, **100** (1967).
- (8) K. R. Dixon, D. W. A. Sharp, and A. G. Sharpe, *Inorg. Synth.*, **12**, 232 (1970).
- (9) T. G. Harrison, H. H. Patterson, and J. J. Godfrey, *Inorg. Chem.*, **15**, 1291 (1976).
- (10) J. S. Griffith, "The Theory of Transition Metal Ions", Cambridge University Press, New York, N.Y., 1961.
- (11) K. A. Schroeder, *J. Chem. Phys.*, **37**, 2553 (1962).
- (12) Y. Tanabe and S. Sugano, *J. Phys. Soc. Jpn.*, **9**, 753 (1954).
- (13) F. A. Cotton and C. B. Harris, *Inorg. Chem.*, **6**, 376 (1967).
- (14) C. E. Moore, *Natl. Bur. Stand. (U.S.)*, *Circ.*, No. 467, Vol. I, II, III, 1949, 1952, 1958.
- (15) P. C. Jordan, H. H. Patterson, and P. B. Dorain, *J. Chem. Phys.*, **49**, 3858 (1968).
- (16) F. A. Cotton, "Chemical Applications of Group Theory", 2nd ed, Wiley-Interscience, New York, N.Y., 1971.
- (17) L. A. Woodward and M. J. Ware, *Spectrochim. Acta*, **19**, 775 (1963).
- (18) P. Stein, V. Miskowski, W. H. Woodruff, J. P. Griffin, K. G. Werner, B. P. Gaber, and T. G. Spiro, *J. Chem. Phys.*, **64**, 2159 (1976).
- (19) I. N. Douglas, J. V. Nicholas, and B. G. Wybourne, *J. Chem. Phys.*, **48**, 1415 (1968).
- (20) H. H. Patterson, J. J. Godfrey, and S. M. Khan, *Inorg. Chem.*, **11**, 2872 (1972).
- (21) J. R. Henderson, M. Muramoto, and R. A. Willett, *J. Chem. Phys.*, **41**, 580 (1964).
- (22) The Franck-Condon factors are available on request from H.H.P.